How to cite: *Angew. Chem. Int. Ed.* **2023**, *62*, e202309981
doi.org/10.1002/anie.202309981

NMR Spectroscopy

Residual-Chemical-Shift-Anisotropy-Based Enantiodifferentiation in Lyotropic Liquid Crystalline Phases Based on Helically Chiral Polyacetylenes

Juan Carlos Fuentes-Monteverde, Markus Noll, Akhi Das, Stefan Immel, Michael Reggelin, Christian Griesinger, and Nilamoni Nath**

Abstract: Anisotropic NMR spectroscopy, revealing residual dipolar couplings (RDCs) and residual chemical shift anisotropies (RCSAs) has emerged as a powerful tool to determine the configurations of synthetic and complex natural compounds. The deduction of the absolute in addition to the relative configuration is one of the primary goals in the field. Therefore, the investigation of the enantiodiscriminating capabilities of chiral alignment media becomes essential. While RDCs and RCSAs are now used for the determination of the relative configuration routinely, RCSAs have not been measured in chiral alignment media such as chiral liquid crystals. Herein, we present this application by measuring RCSAs for chiral analytes such as indanol and isopinocampheol in the lyotropic liquid crystalline phase of an L-valine derived helically chiral polyacetylenes. We have also demonstrated that a single 1D ^{13}C–{^{1}H} NMR spectrum suffices to get the RCSAs circumventing the necessity to acquire two spectra at two alignment conditions.

[*] Dr. J. C. Fuentes-Monteverde, Prof. Dr. C. Griesinger
Max Planck Institute for Multidisciplinary Sciences
Department of NMR-Based Structural Biology
Am Fassberg 11, 37077 Göttingen (Germany)
E-mail: cigr@mpinat.mpg.de

A. Das, Dr. N. Nath
Department of Chemistry
Gauhati University
Guwahati, Jalukbari-781014 (India)
E-mail: nilamoni.nath@gmail.com

Dr. M. Noll, Dr. S. Immel, Prof. Dr. M. Reggelin
Department of Chemistry,
Technical University of Darmstadt,
Alarich Weiss Straße 4, 64287 Darmstadt (Germany)

Introduction

Anisotropic NMR spectroscopy has emerged as a powerful structure determination tool to determine the configurations and conformations of synthetic as well as natural compounds.[1] In some cases, anisotropic data was even successful to determine unknown constitutions.[1a,2] Importantly, residual dipolar couplings (RDCs) have been utilized to determine configurations for molecules that have stereogenic centers separated by several bonds.[1b,3] In cases, when conventional NMR restraints based on *J*-coupling constants,[4] NOEs,[5] and, less frequently, cross-correlated relaxation[6] cannot determine the configuration of some of these molecules, the application of RDC data is a valuable supplement to improve the probability of a correct structural assignment. Although residual chemical shift anisotropies (RCSAs) are the most sensitive anisotropic NMR parameters they are much less exploited in structure elucidation than RDCs.[7] This is mainly due to the fact that reliable measurements of RCSAs and their subsequent application in small molecules has been achieved only since 2016.[1a,7b–c,8] Access to RDCs and RCSAs relies on the generation of anisotropic environments by using a so-called alignment medium.[9] The two main classes of alignment media consist of either a chemically cross-linked polymeric gel[7b,10] or lyotropic liquid crystalline (LLC) phases based on polypeptides,[11] polyacetylenes[12] and polyisocyanides.[13] These media disrupt the isotropy of molecular tumbling thereby imposing a favored orientation onto the analyte that can be described by an alignment tensor. RDCs and recently RCSAs measured from these media have been mostly used to determine *relative* configurations. In terms of the future goal of using RDCs and RCSAs to deduce *absolute* configurations, it is critical to align the analyte in an enantiodifferentiating medium with uniform configuration. Because of the diastereomorphous interactions of such media with chiral analytes, they can align the respective enantiomers differently.[14] Consequently, different RDCs or RCSAs can be measured thereby resulting in a distinction between the enantiomers. In the last decade, several groups reported a good number of chiral alignment media that satisfy this criterion.[10d–f,12c–e,13b,15] These media are chiral LLC phases derived from various polymers such as poly-γ-benzyl-L/D-glutamate (PBLG/PBDG),[10d,11,16] poly-γ-ethyl-L/D-glutamate (PELG/PEDG),[17] polyguanidines,[18] polyisocyanides,[13a–b,15b,19] and polyphenylacetylenes

(PPAs).[12,20] Except for PBLG, most of the alignment media induce sufficiently weak alignment to deliver simple extraction of RDCs. The RDCs of several analytes were measured in these media demonstrating their enantiodiscrimination capabilities. In the case of PBLG, the RDC measurement may be hampered due to its strong alignment.[21] However, groups of Courtieu and Lesot have extensively used the PBLG medium using residual quadrupolar couplings for enantiodiscrimination when isotropic NMR falls short.[11b,22] They have also utilized ^{13}C RCSA difference of enantiomers for enantiodiscrimination using 1D ^{13}C–{^{1}H} NMR spectra.[23] Carbon RCSAs were measured using chiral LLC of the oligopeptide AAKLVFF. Yet, low enantiodiscrimination was found for the only single compound studied.[24] As far as the use of gels are concerned, Luy and co-workers have demonstrated the utility of stretched gelatin gel for the distinction of enantiomers in polar solvents.[10f] Moreover, chiral polyacrylamide-based gels were also utilized for the differentiation of chiral amines.[10e]

Both anisotropic parameters, i.e. RDCs and RCSAs, are determined by the same alignment tensor. While RCSAs encode relative orientational information of individual atoms, RDCs provide the same for bond vectors mostly between a heteroatom and a proton across a single bond. Under certain conditions, the measurement of RCSAs is simpler and more sensitive than that of RDCs, which is why their measurement can be advantageous. Moreover, sometimes the number of RDCs is too small when molecules have numerous bonds that are parallel to each other producing identical RDCs or when they lack protons. These shortcomings of RDCs can be bypassed with RCSAs. Herein we would like to describe the first application of RCSAs to differentiate the enantiomers of chiral analytes oriented in a lyotropic liquid crystalline phase of a helically chiral polymer.

For a number of reasons, helically-chiral polyacetylenes and polyisonitriles have proven superior to PBLG as chiral alignment media[12c–d] for enantiodiscrimination[12e] First, these media afford sharp lines resulting in accurate RDCs. Second, the biphasic nature of a polyisonitrile close to the critical concentration to reach the anisotropic state allows for the measurement of RDCs from a single sample.[13b]

Biphasic behaviour of liquid crystals of PBLG was observed previously and used to measure ^{13}C RCSAs in a single carbon NMR experiment for configuration determination problems.[25] Given the fact that this biphasic behaviour also occurs for polyacetylenes, we expected that the simultaneous determination of isotropic and anisotropic data should be possible with the polyacetylenes as well. The enantiodiscriminating properties of a polyacetylene liquid crystal bearing valine-derived sidechains (PLA) has been already studied for eleven different analytes belonging to five different compound classes including hydrocarbons by comparing experimentally distinguishable RDC values as well as intertensor angles between the RDC-derived alignment tensors.[12d] Recently, this enantiodifferentiating effect has been demonstrated with a serine-derived polyacetylene using RQCs.[20] A most remarkable case of enantiodifferentiating orientation occurs with the enantiomers of the hydrocarbon 3-methylhexane. Despite the fact that the substituents attached to the stereogenic carbon differ only by one carbon each, 17 out of 20 quadrupolar doublets have been observed in a ^{2}H NMR study.[12e] In contrast, RCSA based enantiodiscrimination studies are yet to be conducted in a polyacetylene based LLC-phase. For this purpose, we herein used L-valine derived polyphenylacetylene (PLA) to collect carbon RCSA data for the enantiomers of the two chiral molecules indanol and isopinocampheol (IPC). We also evaluated the enantiodiscriminating capabilities of the LLC phase by inspecting the different order tensor orientations of the enantiomers.

Method section

The PLA employed in this work was synthesized using TPV Rh-catalyst.[12e] At a concentration of 17 % (W_{PLA}) in $CDCl_3$, PLA forms a biphasic mixture with the solvent in isotropic as well as anisotropic environments as judged from the simultaneous observation of a ^{2}H-singlet from the isotropic phase and a quadrupolar doublet ($\Delta\nu_Q = 65.9$ Hz) from the anisotropic phase (Figure 1a). The critical concentration (cc) of PLA and other LLC-phase forming polymers is dependent on several factors: a) parameters such as polymer charge, molecular weight and distribution are subject to small variations leading to changes in the cc, b) the amount of analyte present in the sample changes the cc, and c) especially with $CDCl_3$, an additional factor may be spurious amounts of hydrochloric acid from the light induced decomposition of this solvent. As the critical concentration of the polymer depends on the presence or absence of the analyte, we prepared the sample by adding PLA to the solution of the analyte dissolved in $CDCl_3$ until the biphasic state (visible phase boundary) has been reached. This biphasic system allows the measurement of RCSAs in standard 2/3/5 mm NMR tubes without the need for special equipment.

As shown in Figure 1(b), the 1D ^{13}C–{^{1}H} NMR spectrum of the analyte at 295 K shows two resonances for each carbon. Thus, the spectrum consists of two sub-spectra, one spectrum referring to the isotropic environment of the sample and the other to the anisotropic environment of the sample. The chemical shift difference between these two sub-spectra is caused not only by the RCSAs but also by changes in the overall magnetic susceptibility of the sample. The latter effect can be removed by referencing as the overall magnetic susceptibility affects all the carbon resonances in the identical way.[7a] The referencing can be executed in several ways, viz., by taking one atom of the analyte,[7b] TMS signal[7b] or even the solvent signal[26] If two sub-spectra are referenced at any resonance of the analyte, then the said atom will have a zero RCSA value. It has been found that choice of the resonance for reference does not change the results.[27] The relative concentration of the solvent chloroform in anisotropic and isotropic medium can be estimated from its deuterium spectrum as depicted in Figure 1a. Each of the anisotropic quadrupolar doublet lines has the same intensity as the isotropic singlet (Figure 1a),

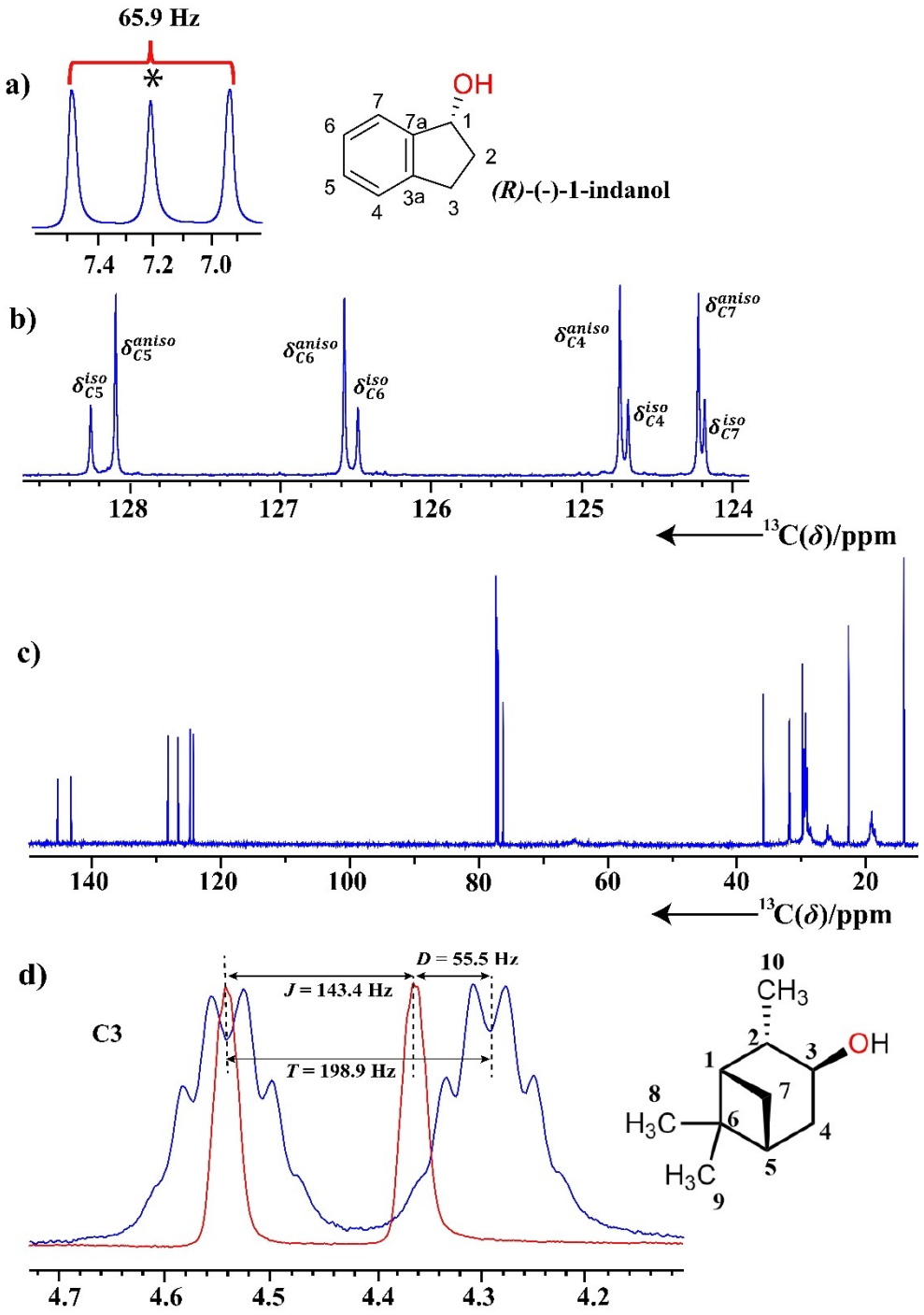

Figure 1. (a) 1D ^{2}H NMR spectrum of $CDCl_3$ in the (*R*)-(−)-1-indanol sample aligned in the LLC phase of L-valine derived polyacetylene (PLA). The splitting fork over the deuterium peaks of $CDCl_3$ indicates the quadrupolar doublet while the central resonance (*) indicates the presence of isotropic phase. The spectrum was recorded at 295 K. b) 1D $^{13}C–\{^{1}H\}$ NMR spectrum of *R*-indanol which was measured in an 800 MHz spectrometer equipped with a cryoprobe. For visual clarity of the isotropic and anisotropic signals of each carbon resonances, expansion of a part of the complete 1D carbon spectrum (c) in the range of 120–130 ppm is shown in (b). For each carbon, peaks with lower and higher intensities correspond to isotropic and anisotropic signals, respectively. The isotropic and anisotropic signals of carbons C5, C6, C4 and C7 are also labelled from left to right in (b). (d) F_2 slices extracted from proton decoupled $^{1}H–^{13}C$ CLIP HSQC spectra of (+)-IPC in anisotropic (blue trace) and isotropic medium (red trace) for C3.

hence the anisotropic phase has double concentration of the isotropic phase. If δ_i^{iso} and δ_i^{aniso} are the chemical shifts from the i^{th} nucleus in isotropic and anisotropic phases, respectively, the RCSAs can be read from the spectra using Equation (1):

$$RCSA_i = \left(\delta_i^{aniso} - \delta_{ref}^{aniso}\right) - \left(\delta_i^{iso} - \delta_{ref}^{iso}\right) \quad (1)$$

where, δ_{ref} is the chemical shift of a reference carbon signal. For referencing, any arbitrary carbon spin of the molecule can be used. Further, the LLC-phase loses its anisotropic fraction to reach a complete isotropic state with increasing temperature. As the sample shows the anisotropic signals at 310 K and isotropic signals at 315 K and 320 K, RCSAs can also be obtained from the following Equation (2):

$$RCSA_i = \delta_i^{aniso,\ 310K} - 2\delta_i^{iso,\ 315K} + \delta_i^{iso,\ 320K} \quad (2)$$

To determine the alignment tensors of the enantiomers, the experimentally observed RCSA values are fitted using singular value decomposition (SVD) together with the Density Functional Theory (DFT) calculated chemical shift anisotropy (CSA) tensors using either MSpin software[28] or ConArch$^+$.[1j,29] The quality of the fit is determined from the Cornilescu Q factor.[30] The DFT based chemical shift anisotropy tensors are calculated from the most commonly used Gauge-Independent Atomic Orbital (GIAO) based methods using *Gaussian* 16.[31] The solvents are modelled using the IEF-PCM[32] model with chloroform solvent parameters. The enantiodiscriminating effect is expressed through generalized cosine β values (GCB) which are equal to normalized scalar products between alignment tensors.[33] This relationship is defined as:

$$cos(\beta) = \frac{\langle A_R^{RCSA}, A_S^{RCSA}\rangle_F}{\|A_R^{RCSA}\|_2 \|A_S^{RCSA}\|_2} \quad (3)$$

Where $\langle A_R^{RCSA}, A_S^{RCSA}\rangle_F$ represents the Frobenius inner product between the RCSA-derived alignment tensors of the (*R/S*)-enantiomers and $\|A_R^{RCSA}\|_2$ and $\|A_S^{RCSA}\|_2$ are the Frobenius norms. The Frobenius inner product of alignment tensors is computed as:

$$\langle A_R^{RCSA}, A_S^{RCSA}\rangle_F = \sum_{k,l=\{x,y,z\}} A_{kl}^R A_{kl}^S \quad (4)$$

while the norm of the matrices is computed due to the symmetric character of the alignment tensor as:

$$\|A_R^{RCSA}\|_2 = \left(\sum_{k=\{x,y,z\}} |A_{kk}^R|^2\right)^{1/2} \quad (5)$$

$$\|A_S^{RCSA}\|_2 = \left(\sum_{k=\{x,y,z\}} |A_{kk}^S|^2\right)^{1/2} \quad (6)$$

Herein, β is the angle between the two alignment tensors. A normalized scalar product of one (1) indicates exact co-linearity of the tensors whereas a zero (0) value means that tensors are perpendicular to each other. This implies that the enantiodiscriminating effect can be estimated based on the β angle (intertensor angle) from the alignment tensors of the enantiomers. Because of the trigonometric relationship, $\cos(180^\circ - \beta) = -\cos(\beta)$, the absolute value of the cosine β can only be between 0 and 1. Therefore, we report the enantiodifferentiation only by cosine β value. Any significant deviation of GCB values from one indicates enantiodiscrimination, the more it deviates from 1 the better the discrimination.

It should be also mentioned that previously for the biphasic polyacetylenes, spatially selectively excited CLIP-HSQC experiment has been utilized to extract the RDCs from a single sample.[13b] However, the spatially and selective experiments suffer from poor sensitivity. It has been found that the highly sensitive F_2-coupled HSQC experiment can be used to extract the RDCs from a single biphasic sample. As an example, one of the F_2 traces extracted from proton decoupled ^{1}H–^{13}C CLIP HSQC spectra of (+)-IPC in anisotropic (blue trace) and isotropic (red trace) phases demonstrated in Figure 1d.

Results and Discussion

R-indanol dissolved in the biphasic system mentioned above was investigated first. The observation of one inner singlet and one outer doublet of the solvent chloroform (Figure 1a) confirms the presence of both an isotropic and an anisotropic phases from a single sample. In essence, the sample contains two well separated phases: one with the PLA concentration below and the other with a polymer concentration well above the critical concentration (Figure S1 in supplement). As reported in similar findings for PBLG liquid crystal[25] and gel,[7b] this observation leads to the fact that RCSAs are measurable from a single 1D ^{13}C–{^{1}H} spectrum provided both isotropic and anisotropic signals are present with sufficient signal-to-noise ratios and chemical shift separation. As expected, Figure 1b shows that the 1D ^{13}C–{^{1}H} spectrum contains two sets of signals for each carbon resonance. As can clearly be seen from the spectrum, for alignment with a polyacetylene mass fraction (W_{PLA}) of 17 % in $CDCl_3$, WALTZ decoupling applied during acquisition is sufficient to remove the combined scalar and dipolar CH-couplings ($^1T_{CH}$). Most notably, very sharp ^{13}C resonances (spectral linewidths of 2–3 Hz) can be observed. Signal-to-noise ratios obtained are in the range of 20 to 50. Therefore, parallel to the ^{13}C spectrum in isotropic liquid, the corresponding chemical shift positions from the anisotropic phase are easily readable. From the integration values of the ^{2}H resonances, it is found that the intensity of the isotropic singlet is approximately 46 % of the anisotropic doublet signal. Thus, a carbon signal of lower intensity comes from the isotropic phase of the sample while the signal with higher intensity belongs to the anisotropic phase.

The RCSA values of *R*-indanol were extracted using Equation (1) and C7a as reference carbon resonance. The RCSA values obtained cover a favorable range of −3.9 to 57.5 Hz at a carbon resonance frequency of 200 MHz. For RCSA data interpretation, carbon CSA tensors computed for the correct structural model are essential. Following standard computational chemistry protocols, we have found

that there are two structural models (conformers). They are called conformer "A", in which C-2 is up and OH group is pseudo-axial, and conformer "B", in which C-2 is down and OH group is pseudo-equatorial. The DFT-optimized geometries of these conformers are presented in Figure 2a. Both molecular models were obtained following DFT optimization at mPW1PW91/6-31+G(2d,p) level with chloroform solvent parameters. It is found that the model "B" turned out to be even very slightly more stable than the model "A". The energy difference between them is −0.4 kcal/mol. The CSA tensors of DFT models of *S*-indanol were then computed using GIAO method at DFT mPW1PW91/6-311+G (2d,p) level.

As both the enantiomers of indanol are available, our strategy is based on two samples of enantiomeric analytes. Both samples were prepared in PLA, thus generating diastereomorphous interactions between the stereochemically constant polymer and the enantiomers of the analyte. For sample preparation, we utilized the same composition that was used for *R*-indanol. As previously noted, RCSAs were extracted for *S*-indanol from 1D $^{13}C–\{^1H\}$ NMR spectrum recorded at 295 K. RCSA values ranged from −11.6 to 23.5 Hz. As the polymer concentration in the *R*-indanol sample is slightly different compared to the other enantiomer, RCSA values were normalized by the ratio of the quadrupolar splitting of the two enantiomeric samples ($\Delta\nu_Q(S)/\Delta\nu_Q(R)=0.87$). As can clearly be seen from the scatter plot in Figure 2b, RCSA values for *S*-indanol (RCSAs on the y-axis) and *R*-indanol (RCSAs on the x-axis) are different. The bar plot of the differential RCSA values of enantiomers is also provided in Figure S2 in supplement.

As previously observed with RDCs of other analytes, the use of RCSAs also indicates the enantiodifferentiation capabilities of the polyacetylene based liquid crystal. For quantitative evaluation of differential orientations of the enantiomeric analytes, we calculated the generalized cos(*β*) value between their RCSA-derived order tensors. Any cos(*β*) value significantly deviating from 1 indicates enantiodiscrimination. Therefore, RCSA data obtained for *S*-indanol were applied for order tensor calculations using MSpin software. The SVD-fit of RCSA values into the CSA tensor furnished a lower *Q* factor of 0.123 for model "B" of *S*-indanol indicating a good congruence of experimental and calculated RCSA. However, high energy structural model "A" furnished relatively higher *Q* factor (0.241). As the model "B" provides lower *Q* factor, therefore, its order tensor parameters are used to calculate generalized cos(*β*) values (GCB). The comparison of the order tensors leads to a GCB value of 0.78. For comparison, RDC-based GCBs on some other analytes using polyacetylene liquid crystals can be used. As examples, GCBs for some investigated analytes are, α-pinene: 0.95, fructose-acetonide: 0.63 and perillaldehyde: 0.82, β-caryophyllene: 0.98, carvone: 0.95 and camphor: 0.98.[12d]

Considering these values, the observed GCB of indanol indicates a substantial degree of enantiodiscrimination. The pictorial representation of alignment tensor 3D surface and the different orientations of the principal axes of the alignment tensor of the *R*- and *S*-indanol are depicted in Figure S3 in supplement. In these pictorial representations, the least ordered A_x axes are kept in the same direction so that the difference in other orientations becomes more evident. Moreover, the most ordered axis is negative for *R*-indanol while it is positive for *S*-indanol. The orientational properties of both enantiomers are provided in Table S5 in the supplement.

We have also fit the RCSA data to both structural models using a single tensor. This furnished a *Q* factor of 0.092 and 0.099 for the RCSA data of *R*- and *S*-indanol, respectively and leads to a 66.1:33.9 population mixture (model B:A).

As a next example, we measured ^{13}C RCSAs for isopinocampheol (IPC). The choice of this molecule is based

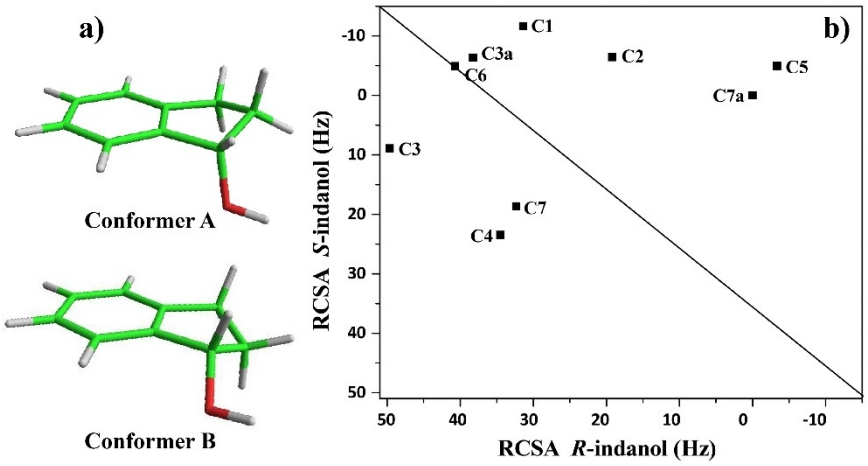

Figure 2. (a) DFT-optimized structural models "A" and "B" of *S*-indanol. (b) Scatter plot of the residual chemical shift anisotropy (RCSA) values for *S*-indanol and *R*-indanol aligned in PLA. To extract the RCSA values for the enantiomeric analytes, both the sub-spectra corresponding to isotropic and anisotropic signals are referenced at carbon signal C7a. The RCSA values for different carbons are marked in the scatter plot. It should be noted that the alignment tensors of *R*- and *S*-indanol have different orientations relative to each other with a GCB value of 0.78 between them.

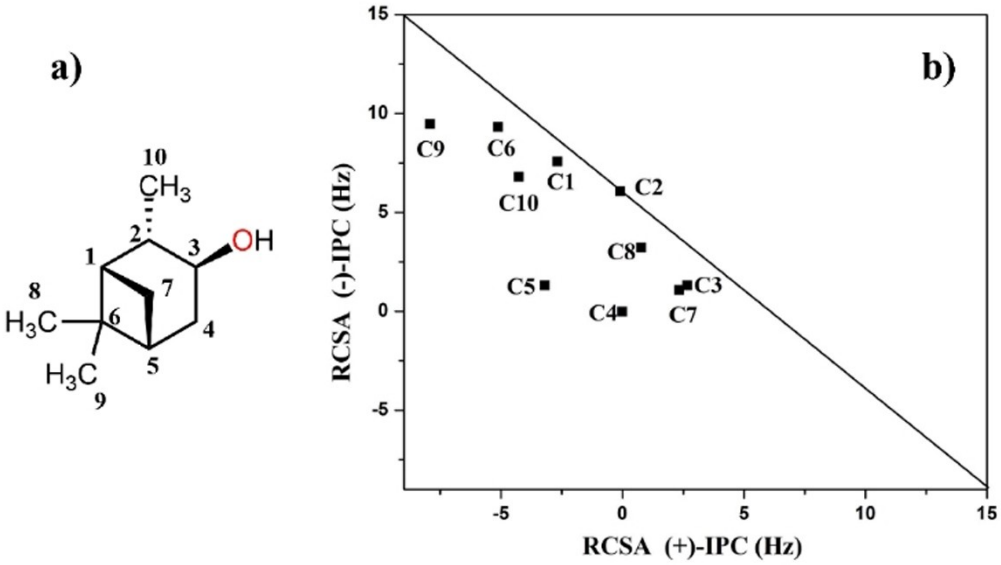

Figure 3. (a) Molecular structure of (+)-IPC with atomic numbering. (b) Scatter plot of the residual chemical shift anisotropy (RCSA) values for (+)-IPC and (−)-IPC aligned in PLA. The RCSA values for different carbons are marked in the scatter plot.

mainly on two facts. First, its rigid structure facilitates the data analysis and second, there are several RDC-based studies demonstrating enantiodiscrimination in several chiral liquid crystals including PLA.[20,34]

To compare the RCSA-based enantiodiscriminating capabilities of the polymer, we again prepared two separate samples of (+)-IPC and (−)-IPC using W_{PLA} of 17 % in $CDCl_3$. RCSAs were measured by employing Eqn. (2). As expected and shown in Figure 3, measured RCSA values were different for these two samples. The RCSA values ranged from −7.9 to 2.7 Hz for (−)-IPC while values were in between 1.1 to 9.5 Hz for (+)-IPC. This finding indicates that (+)- and (−)-IPC orient very differently relative to the axis of the magnetic field. To obtain more quantitative insights, we performed the SVD analysis of the measured RCSA values for the enantiomers. For the SVD fitting, carbon CSA tensors of (−)-IPC computed by GIAO-based methods using DFT level at B3LYP/6-311 + G(2d,p) were employed for both data sets. The SVD-fitting of RCSA data of (−)-IPC to the CSA tensors results in a *Q* factor of 0.109. Similarly, the same *Q* factor is obtained for the SVD fitting of the RCSA data of (+)-IPC. The intertensor cos(*β*) value between the RCSA-derived tensors of (+)-IPC and (−)-IPC was then calculated and the GCB of the alignment tensors was found to be −0.44. This large negative GCB indicates that very significant enantiodifferentiation is taking place. It may be noted that similar to the RCSA-based results, large enantiodiscrimination was also found for the previously analyzed RDC data measured in liquid crystals of PLA.[12d] It should be mentioned that we did not measure the proton RCSAs that are even more sensitive than the ^{13}C RCSAs, introduced for enantiodiscrimination in this work. ^{1}H RCSA measurement requires deuterated alignment media for small amounts of analyte.[7c] This seems to be feasible for polyacetylenes such that, measuring ^{1}H RCSAs at microgram level will become feasible in the future work.

Conclusion

Exploiting the biphasic behaviour of a helically chiral polyarylacetylene based liquid crystal (PLA), it has been shown that ^{13}C-RCSAs can be measured from the isotropic and ansiotropic signals under a single alignment condition and as expected[12e] enantiodiscrimination is better than with PBLG. Thus, with PLA ^{13}C RCSAs can be robustly used to enantiodiscriminate organic molecules. Using the example of two chiral low molecular weight compounds, IPC and indanol, we were able to demonstarte that the extraction of ^{13}C-RCSAs from simple proton decoupled ^{13}C spectra was possible in a precise and accurate manner. Moreover, due to the uniform helicity of the polymer forming the LLC-phase, substantial enantiodifferentiation occurs as judged from the GCB value of the alignment tensors calculated for the respective enantiomers of the analytes. Especially for proton-poor molecules with quaternary carbons or in cases when the alignment is too strong to measure RDCs, ^{13}C-RCSAs represent a valuable additional source of information to solve structural problems which are reluctant to be solved by other means. Future work will allow the usage of ^{1}H RCSAs in PLA once it is deuterated.

Acknowledgements

N.N. gratefully acknowledges the financial support by SERB, New Delhi for CRG Grant with File No. CRG/2022/005993. This work was funded by the DFG (Gr1211/19-1 and Re1007/9-1)/CAPES 418729698 project and the Max

Planck Society. Open Access funding enabled and organized by Projekt DEAL.

Conflict of Interest

The authors declare no conflict of interest.

Data Availability Statement

The data that support the findings of this study are available from the corresponding author upon reasonable request.

Keywords: Chiral Liquid Crystals · NMR Spectroscopy · Polyacetylenes · Residual Chemical Shift Anisotropy · Enantiodiscrimination

[1] a) Y. Liu, J. Sauri, E. Mevers, M. W. Peczuh, H. Hiemstra, J. Clardy, G. E. Martin, R. T. Williamson, *Science* **2017**, *356*, eaam 5349; b) P. Trigo-Mouriño, A. Navarro-Vázquez, J. Ying, R. R. Gil, A. Bax, *Angew. Chem. Int. Ed.* **2011**, *50*, 7576–7580; c) G. Kummerlöwe, B. Luy, *Annu. Rep. Nmr Spectrosc, Vol. 68* (Ed.: G. A. Webb), Academic Press **2009**, pp. 193–232; d) H. Sun, U. M. Reinscheid, E. L. Whitson, E. J. d'Auvergne, C. M. Ireland, A. Navarro-Vázquez, C. Griesinger, *J. Am. Chem. Soc.* **2011**, *133*, 14629–14636; e) B. Böttcher, C. M. Thiele, *eMagRes, Vol. 1*, Wiley, Hoboken **2012**, pp. 169–180; f) G. Cornilescu, R. F. Ramos Alvarenga, T. P. Wyche, T. S. Bugni, R. R. Gil, C. C. Cornilescu, W. M. Westler, J. L. Markley, C. D. Schwieters, *ACS Chem. Biol.* **2017**, *12*, 2157–2163; g) E. Sager, P. Tzvetkova, A. D. Gossert, P. Piechon, B. Luy, *Chem. Eur. J.* **2020**, *26*, 14435–14444; h) P. Lesot, R. R. Gil, P. Berdagué, A. Navarro-Vázquez, *J. Nat. Prod.* **2020**, *83*, 3141–3148; i) M. Köck, M. Reggelin, S. Immel, *Mar. Drugs* **2021**,*19*, 283–298; j) S. Immel, M. Köck, M. Reggelin, *J. Nat. Prod.* **2022**, *85*, 1837–1849.

[2] G. Kummerlöwe, B. Crone, M. Kretschmer, S. F. Kirsch, B. Luy, *Angew. Chem. Int. Ed.* **2011**, *50*, 2643–2645.

[3] a) N. Nath, E. d'Auvergne, C. Griesinger, *Angew. Chem. Int. Ed.* **2015**, *54*, 12706–12710; b) L. F. Gil-Silva, R. Santamaría-Fernández, A. Navarro-Vázquez, R. R. Gil, *Chem. Eur. J.* **2016**, *22*, 472–476.

[4] a) M. Karplus, *J. Chem. Phys.* **1959**, *30*, 11–15; b) C. A. G. Haasnoot, F. A. A. M. de Leeuw, C. Altona, *Tetrahedron* **1980**, *36*, 2783–2792.

[5] F. A. L. Anet, A. J. R. Bourn, *J. Am. Chem. Soc.* **1965**, *87*, 5250–5251.

[6] B. Reif, M. Hennig, C. Griesinger, *Science* **1997**, *276*, 1230–1233.

[7] a) F. Hallwass, M. Schmidt, H. Sun, A. Mazur, G. Kummerlöwe, B. Luy, A. Navarro-Vázquez, C. Griesinger, U. M. Reinscheid, *Angew. Chem. Int. Ed.* **2011**, *50*, 9487–9490; b) N. Nath, M. Schmidt, R. R. Gil, R. T. Williamson, G. E. Martin, A. Navarro-Vázquez, C. Griesinger, Y. Liu, *J. Am. Chem. Soc.* **2016**, *138*, 9548–9556; c) N. Nath, J. C. Fuentes-Monteverde, D. Pech-Puch, J. Rodríguez, C. Jiménez, M. Noll, A. Kreiter, M. Reggelin, A. Navarro-Vázquez, C. Griesinger, *Nat. Commun.* **2020**, *11*, 4372–4381.

[8] a) Y. Liu, A. Navarro-Vázquez, R. R. Gil, C. Griesinger, G. E. Martin, R. T. Williamson, *Nat. Protoc.* **2019**, *14*, 217–247; b) Y. Liu, R. D. Cohen, K. R. Gustafson, G. E. Martin, R. T. Williamson, *Chem. Commun.* **2018**, *54*, 4254–4257; c) E. Hellemann, R. R. Gil, *Chem. Eur. J.* **2018**, *24*, 3689–3693; d) I. E. Ndukwe, A. Brunskill, D. R. Gauthier, Y.-L. Zhong, G. E. Martin, R. T. Williamson, M. Reibarkh, Y. Liu, *Org. Lett.* **2019**, *21*, 4072–4076.

[9] N. Tjandra, A. Bax, *Science* **1997**, *278*, 1111–1114.

[10] a) J. C. Freudenberger, P. Spiteller, R. Bauer, H. Kessler, B. Luy, *J. Am. Chem. Soc.* **2004**, *126*, 14690–14691; b) R. R. Gil, C. Gayathri, N. V. Tsarevsky, K. Matyjaszewski, *J. Org. Chem.* **2008**, *73*, 840–848; c) G. Kummerlowe, M. U. Kiran, B. Luy, *Chem. Eur. J.* **2009**, *15*, 12192–12195; d) T. Montag, C. M. Thiele, *Chem. Eur. J.* **2013**, *19*, 2271–2274; e) M. Schmidt, H. Sun, A. Leonov, C. Griesinger, U. M. Reinscheid, *Magn. Reson. Chem.* **2012**, *50*, S38–S44; f) K. Kobzar, H. Kessler, B. Luy, *Angew. Chem. Int. Ed.* **2005**, *44*, 3145–3147.

[11] a) C. Aroulanda, P. Lesot, *Chirality* **2022**, *34*, 182–244; b) P. Lesot, C. Aroulanda, P. Berdague, A. Meddour, D. Merlet, J. Farjon, N. Giraud, O. Lafon, *Prog. Nucl. Magn. Reson. Spectrosc.* **2020**, *116*, 85–154.

[12] a) K. Okoshi, K. Sakajiri, J. Kumaki, E. Yashima, *Macromolecules* **2005**, *38*, 4061–4064; b) M. Dama, S. Berger, *Tetrahedron Lett.* **2012**, *53*, 6439–6442; c) N. C. Meyer, A. Krupp, V. Schmidts, C. M. Thiele, M. Reggelin, *Angew. Chem. Int. Ed.* **2012**, *51*, 8334–8338; d) A. Krupp, M. Noll, M. Reggelin, *Magn. Reson. Chem.* **2021**, *59*, 577–586; e) P. Lesot, P. Berdagué, A. Meddour, A. Kreiter, M. Noll, M. Reggelin, *ChemPlusChem* **2019**, *84*, 144–153.

[13] a) M. Dama, S. Berger, *Org. Lett.* **2012**, *14*, 241–243; b) M. Reller, S. Wesp, M. R. M. Koos, M. Reggelin, B. Luy, *Chem. Eur. J.* **2017**, *23*, 13351–13359; c) K. Okoshi, K. Nagai, T. Kajitani, S. I. Sakurai, E. Yashima, *Macromolecules* **2008**, *41*, 7752–7754.

[14] P. Lesot, M. Sarfati, J. Courtieu, *Chem. Eur. J.* **2003**, *9*, 1724–1745.

[15] a) G.-W. Li, X.-J. Wang, X. Lei, N. Liu, Z.-Q. Wu, *Macromol. Rapid Commun.* **2022**, *43*, 2100898; b) N. Liu, L. Zhou, Z. Q. Wu, *Acc. Chem. Res.* **2021**, *54*, 3953–3967.

[16] A. Marx, C. Thiele, *Chem. Eur. J.* **2009**, *15*, 254–260.

[17] S. Hansmann, T. Larem, C. M. Thiele, *Eur. J. Org. Chem.* **2016**, 1324–1329.

[18] L. Arnold, A. Marx, C. Thiele, M. Reggelin, *Chem. Eur. J.* **2010**, *16*, 10342–10346.

[19] M. K. Reggelin, S. Wesp, K. Wolf, S. Immel, *ChemPlusChem* **2022**, *87*, e202100507.

[20] P. Berdagué, B. Gouilleux, M. Noll, S. Immel, M. Reggelin, P. Lesot, *Phys. Chem. Chem. Phys.* **2022**, *24*, 7338–7348.

[21] Y. Liu, R. D. Cohen, G. E. Martin, R. T. Williamson, *J. Magn. Reson.* **2018**, *291*, 63–72.

[22] M. Sarfati, P. Lesot, D. Merlet, J. Courtieu, *Chem. Commun.* **2000**, 2069–2081.

[23] A. Meddour, P. Berdague, A. Hedli, J. Courtieu, P. Lesot, *J. Am. Chem. Soc.* **1997**, *119*, 4502–4508.

[24] X.-L. Li, L.-P. Chi, A. Navarro-Vázquez, S. Hwang, P. Schmieder, X.-M. Li, X. Li, S.-Q. Yang, X. Lei, B.-G. Wang, H. Sun, *J. Am. Chem. Soc.* **2020**, *142*, 2301–2309.

[25] M. J. J. Recchia, R. D. Cohen, Y. Liu, E. C. Sherer, J. K. Harper, G. E. Martin, R. T. Williamson, *Org. Lett.* **2020**, *22*, 8850–8854.

[26] D. S. Carvalho, D. G. B. da Silva, F. Hallwass, A. Navarro-Vázquez, *J. Magn. Reson.* **2019**, *302*, 21–27.

[27] A. Das, N. Nath, *Magn. Reson. Chem.* **2021**, *59*, 569–576.

[28] A. Navarro-Vazquez, *Magn. Reson. Chem.* **2012**, *50*, S73–S79.

[29] a) S. Immel, M. Kock, M. Reggelin, *Chem. Eur. J.* **2018**, *24*, 13918–13930; b) S. Immel, M. Kock, M. Reggelin, *Chirality* **2019**, *31*, 384–400; c) S. Immel, M. Köck, M. Reggelin, *J. Am. Chem. Soc.* **2022**, *144*, 6830–6838.

[30] G. Cornilescu, A. Bax, *J. Am. Chem. Soc.* **2000**, *122*, 10143–10154.

[31] Gaussian 16, Revision C.01, M. J. Frisch, G. W. Trucks, H. B. Schlegel, G. E. Scuseria, M. A. Robb, J. R. Cheeseman, G. Scalmani, V. Barone, G. A. Petersson, H. Nakatsuji, X. Li, M. Caricato, A. V. Marenich, J. Bloino, B. G. Janesko, R. Gomperts, B. Mennucci, H. P. Hratchian, J. V. Ortiz, A. F. Izmaylov, J. L. Sonnenberg, Williams, F. Ding, F. Lipparini, F. Egidi, J. Goings, B. Peng, A. Petrone, T. Henderson, D. Ranasinghe, V. G. Zakrzewski, J. Gao, N. Rega, G. Zheng, W. Liang, M. Hada, M. Ehara, K. Toyota, R. Fukuda, J. Hasegawa, M. Ishida, T. Nakajima, Y. Honda, O. Kitao, H. Nakai, T. Vreven, K. Throssell, J. A. Montgomery Jr, J. E. Peralta, F. Ogliaro, M. J. Bearpark, J. J. Heyd, E. N. Brothers, K. N. Kudin, V. N. Staroverov, T. A. Keith, R. Kobayashi, J. Normand, K. Raghavachari, A. P. Rendell, J. C. Burant, S. S. Iyengar, J. Tomasi, M. Cossi, J. M. Millam, M. Klene, C. Adamo, R. Cammi, J. W. Ochterski, R. L. Martin, K. Morokuma, O. Farkas, J. B. Foresman, D. J. Fox, Gaussian, Inc.,Wallingford, CT **2016**.

[32] G. Scalmani, M. J. Frisch, *J. Chem. Phys.* **2010**, *132*, 114110–114125.

[33] a) J. Sass, F. Cordier, A. Hoffmann, M. Rogowski, A. Cousin, J. G. Omichinski, H. Löwen, S. Grzesiek, *J. Am. Chem. Soc.* **1999**, *121*, 2047–2055; b) F. Kramer, M. V. Deshmukh, H. Kessler, S. J. Glaser, *Concepts Magn. Reson. Part A* **2004**, *21A*, 10–21.

[34] M. Tichotová, T. Landovský, J. Lang, S. Jeziorowski, V. Schmidts, M. Kohout, M. Babor, P. Lhoták, C. M. Thiele, H. Dvořáková, *J. Org. Chem.* **2023**, https://doi.org/10.1021/acs.joc.2c02594.

Manuscript received: July 13, 2023
Accepted manuscript online: September 8, 2023
Version of record online: October 13, 2023